

## THE EFFECT OF THE NUMBER OF THE BLADES ON DIFFUSER AUGMENTED WIND TURBINE PERFORMANCE

MOHAMED M. TAKEYELDEIN<sup>1,\*</sup>, I. S. ISHAK<sup>2</sup>, THOLUDIN M. LAZIM<sup>1</sup>

<sup>1</sup>Faculty of Mechanical Engineering, Universiti Teknologi Malaysia,  
81310 Skudai, Johor, Malaysia

<sup>2</sup>UTM Aerolab, Institute for Vehicle System & Engineering, Universiti  
Teknologi Malaysia, 81310, Johor Bahru, Malaysia

\*Corresponding Author: mohamedtakey@outlook.com

### Abstract

Diffuser Augmented Wind Turbine (DAWT) has been acknowledged to accelerate the flow and increase the efficiency of the wind turbine exceeding the Betz limit. However, the flow separation that occurs on the inner walls of DAWT is the main problem unfavorably degrading the DAWT performance. Therefore, this study aimed to assess the possibility of using the number of rotor blades as a passive boundary layer control. In this research, the DAWT design consists of a small wind turbine with a diameter of 0.6m and a compact diffuser shroud. The ratio between the diffuser length and the rotor's diameter is 0.21. This research was conducted using computational fluid dynamics (CFD) simulations via Ansys CFX wherein the result was validated using wind tunnel testing. Analyzing the velocity contours behind the rotor's plane showed that increasing the number of the rotor's blades would augment the kinetic energy at the rotor's tips which helped energize the flow close to the diffuser's inner walls. Consequently, this helped the boundary layer stay attached to the diffuser's walls and avoid separation. Velocity vectors from CFD results showed that the 4-blade DAWT has the flow fully attached to the diffuser at an opening angle of 20° compared to the 3-blade and 2-blade DAWT, which had the flow completely separated at the same opening angle. In conclusion, the findings proved that the number of blades could be used as a passive boundary layer control.

Keywords: CFD, Diffuser augmented wind turbine, Ducted wind turbine, Horizontal axis wind turbine, Wind-lens turbine, Wind tunnel testing.

## 1. Introduction

Diffuser Augmented Wind Turbines (DAWT) have been proven to have enhanced performance compared to bare wind turbines [1, 2]. The efficiency of wind turbines is limited to what is known by the Betz limit, which is 59.3% [3]. Many researchers have demonstrated that adding a diffuser behind the turbine significantly increases power output, exceeding the Betz limit [1, 4].

DAWT mainly consists of a wind turbine shrouded with a diffuser duct as shown in Fig. 1. Increasing the area ratio between the diffuser's inlet and outlet can increase the efficiency of the DAWT. However, flow separation happens at the inner walls of the diffuser walls because of the adverse pressure gradient [5, 6]. Flow separation changes the effective shape of the diffuser, which limits its function [7].

The interaction between the turbine's wake and the flow passing inside the diffuser is critical to DAWT's overall performance [5, 8]. It was noticed in the literature that the turbine's wake mixed with the boundary layer shedding and reduced the separation [4, 5]. Since the number of the rotor's blades influences the energy of the wakes behind the turbine [9], hence it might be used as a parameter to suppress the flow separation.

There is insufficient knowledge about how the number of the blade which influence the turbine's wake energy could be a factor in determining whether the flow separates the diffuser walls. Hence, the primary aim of the research is to investigate the possibility of using the number of rotor blades as a passive boundary layer control. It is achieved by comparing the flow structure at the inner walls of the diffuser using when using 2-blade, 3-blade, and 4-blade rotors.

### 1.1. Brief review of DAWT

Diffuser ducts have been proven to speed up the airspeed in a free flow by suction effect. A diffuser is a duct that serves pressure recovery [10]; which means a pressure difference is created across its length. The diffuser inlet has a pressure lower than the atmosphere, encouraging the upstream air to flow through the diffuser [11]. It is proven that mating a turbine with a diffuser increases the power significantly [12].

The diffuser increases the mass flow rate through the rotor. It causes a pressure gradient downstream after the rotor because the diffuser must end up with sub-atmospheric pressure at its exit; the pressure directly behind the rotor is decreased. Hence, the pressure difference across the turbine increases, which increases the speed of air and hence the power [13, 14].

Wind turbines shrouded with a diffuser are known as Diffuser Augmented Wind Turbines (DAWT) [2]. DAWT's early designs had a long-length diffuser with a large opening angle to ensure a large area ratio between the diffuser inlet and output. On the other hand, the large opening angle creates an adverse pressure gradient within the diffuser walls, leading to flow separation. Flow separation requires boundary layer control mechanisms such as air slots or multistage diffusers, which add to the complexity of their design. [13, 15-17]. The early designs of DAWT have never been upgraded to become a commercial product

because of the complexity added by the boundary layer controllers and the cost added by the long diffuser [1, 11, 17, 18].

Another DAWT design concept introduced by a group of researchers led by Professor Yuji Ohya at Kyushu University called the Wind-lens turbines [1, 11, 17, 18]. A wind lens turbine is a compact ducted wind turbine characterized by a small length-to-diameter ratio of less than 0.4 and a high vertical flange at its rear. The flange holds an essential role in the wind lens concept. It acts as a vortex generator, which produces a low-pressure zone at the back of the wind lens, which finally helps the flow speed up [2, 18].

## 1.2. Influence of the number of Blades on DAWT Performance

Many parameters influence the performance of the DAWT such as the opening angle of the diffuser, the diffuser profile, the back pressure, and the interaction between the flow past the blades and the flow close to the diffuser walls [19-23]. One of the parameters that affect the flow interaction is the rotor's blade number.

By default, most modern horizontal-axis wind turbines have three blades [3]. Two-blade turbines require high RPM to achieve the same power coefficient as the three blades, which increases the noise and the structural vibration because of the imbalance in the moment of inertia. Four-blade turbines could be slightly more efficient than three-blade turbines; however, the increase in power does not justify the cost of the extra blade [3, 24]. Consequently, most DAWT designs use a 3-blade turbine. Table 1 shows earlier designs that use multi-blade rotors instead of 3-blade rotors.

**Table 1. A list of earlier designs that use multi-blade rotors.**

Name/Year	Year	Methodology	Blade number
Wang and Chen [25]	2008	CFD	2-8blades
Chen et al. [26]	2012	Wind tunnel	6 blades
Aranake et al. [1], [4]	2015	CFD	2 blades
Abdelwaly et al. [27]	2019	CFD	2 blades
Asl et al. [28]	2017	Wind tunnel	2-4 blades
Riyanto et al. [29]	2019	Wind tunnel	2-4blades
Nunes et al. [30]	2019	Wind tunnel	4 blades
Agha et al. [31]	2020	Field test	6 blades

Ohya et al. [32] stated that a diffuser with an opening angle of over  $4^\circ$  would be vulnerable to flow separation. However, it was shown using Particle-Image-Velocimetry (PIV) that when the rotor is attached to the diffuser, the opening angle range could be increased to  $12^\circ$ . Hence, the flow separation reduces when the turbine is attached [5].

The diffuser becomes more efficient after attaching the turbine because of the swirling of the wakes, which gives energy to the boundary layer that helps it resist separation because of the adverse pressure inside the diffuser. Hence, a wider angle can be used, which allows a larger area ratio with shorter diffusers. This observation was also noticed by Aranake et al. [1, 4] in their CFD investigation. Hence, it can be assumed that the wakes of the turbine can control the separation.

The number of rotor blades affects the wake's energy and turbulence intensity behind the turbine. Turbines with two blades produce wakes with higher turbulence intensity than a three-bladed rotor. Also, turbines with three blades produce wakes with higher energy than the two blades [3, 9]. The blade's number consequently affects the flow behavior inside the diffuser and the overall shrouded turbine performance [5, 6, 33]. As a result, the turbine's number of blades and solidity may regulate its wake energy; it can be used as a boundary layer control without adding more components.

Chen et al. [26] studied a DAWT with six blades using a wind tunnel; however, the solidity of the same blade changed while keeping the number of blades the same. It was noticed that reducing the solidity improves the augmentation ratio while keeping the area ratio the same. The same phenomenon was noticed by Asl et al. [28] during wind tunnel testing of 9 configurations of shrouded turbines. Asl et al. [28] concluded that the 2-blade turbine had the highest augmentation compared to the 3-blade or 4-blade. Also, reducing the solidity by changing the rotor's angle of attack increased the augmentation ratio.

Increasing the number of blades while keeping the area ratio the same results in blockage of airflow inside the diffuser, which slows down the upcoming flow [25]. Increasing the number of blades reduces the cut-in speed; however, it causes an increase in solidity, which causes a slowdown of the upcoming flow [34]. The number of blades also affects the generator choice since the fewer the number of blades, the higher the RPM. The influence of the number of blades on the flow separation inside the DAWT is investigated in this research.

## 2. DAWT Configuration

The technical drawing of the DAWT configuration is shown in Fig. 1. A detailed description of the diffuser and the bare wind turbine are listed in Tables 2 and 3, respectively.

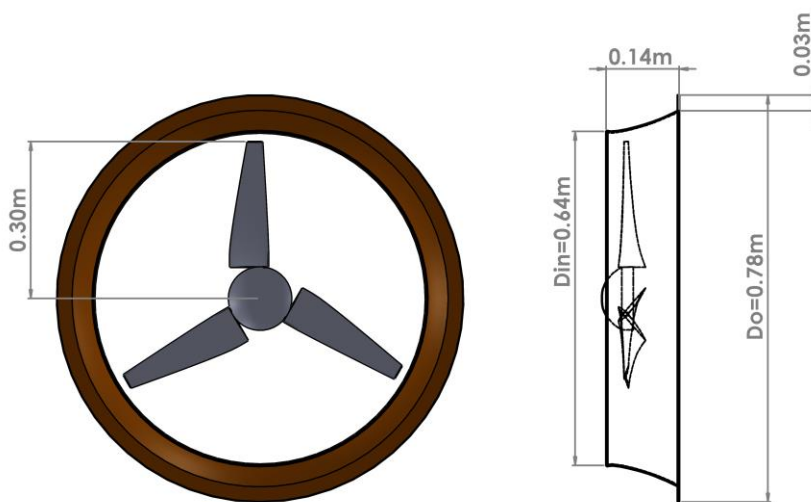


**Fig. 1. A Technical Drawing of the three-blade DAWT.**

**Table 2. A detailed description of the diffuser shroud.**

Inlet Diameter ( $D_{in}$ )	0.64 m
Outlet Diameter ( $D_o$ )	0.78 m
Rotor Diameter ( $D$ )	0.6 m
Diffuser length ( $L$ )	0.14 m
Flange height ( $H$ )	0.03 m
Tolerance between blade tip and diffuser	0.02 m
Opening angle	15°
$L/D$	0.23
Length of diffuser	0.14 m
$D/D_o$	0.6/0.7786
Diffuser profile	Airfoil SD2030

**Table 3. A detailed description of the bare wind turbine**

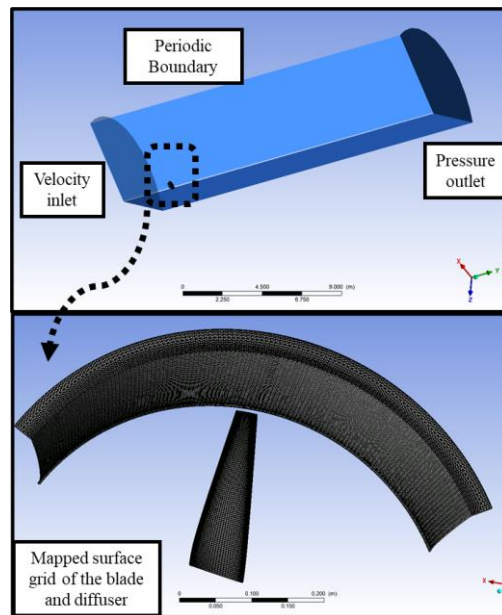
Position (m)	Chord (m)	Twist (°)
0.06	0.09	20
0.09	0.0825	12.2
0.12	0.075	8
0.15	0.0675	5.3
0.18	0.06	3.6
0.21	0.0525	2.3
0.24	0.045	1.3
0.27	0.0375	0.6
0.3	0.03	0

### 3. CFD Simulation Setup

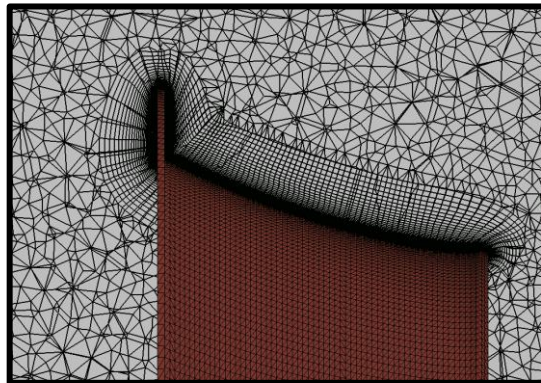
The performance of the bare and DAWT has been investigated using 3D CFD simulation. The Reynolds Averaged Navier-Stokes (RANS) equations were solved using CFX Ansys software. The flow is assumed to be steady and incompressible everywhere. The computational domain is 20 m long, more than thirty-three times the rotor diameter. It has been divided into two zones, as shown in Fig. 2: a rotating domain including the turbine blade, and a stationary zone having the diffuser wall. A C-grid zone with hexahedral structured mesh elements was built along the blade span from root to tip to capture the flow inside the boundary layer. The C-grid that surrounds the blade is seen in Fig. 2(c). The height of the first layer close to the wall surface is chosen as small enough to make sure the dimensionless distance from the wall ( $Y_{plus}$ ) is less than 1. A zone of dense mesh elements is created around the diffuser to capture the pressure gradient that occurs across it. Fig. 2(b) shows inflation layers, which were also created around the diffuser walls to capture the boundary layer. The mesh elements everywhere else in the domain are unstructured 3D tetrahedral cells created using Ansys meshing.

### 4. Wind Tunnel Testing

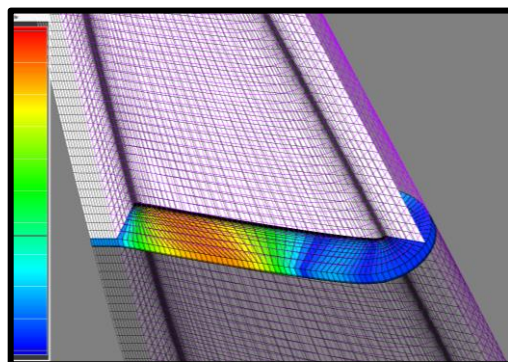
The wind tunnel testing was conducted at the Universiti Teknologi Malaysia's low-speed wind tunnel which is a closed circuit with a test section of 1.5 m (H)  $\times$  2.0 m (W)  $\times$  5.8 m (L); the flow angle is less than 0.15°, and the turbulence intensity is less than 0.04%. The main aim of this experimental work is to calculate the power coefficient vs. tip speed ratio (TSR) of the 3-blade DAWT to validate the CFD model, Fig. 3. The inlet velocity is fixed at 5 m/s. The rotor's rotational speed is controlled by the brake disk system; at the same time, the rotor's torque is measured using the dynamic torque sensor FUTEK TRS605.



(a). Computational domain and boundary conditions.



(b). Inflation layers around the diffuser walls.



(c). C-Grid around the blade.

Fig. 2. Computational grid for the shrouded turbine.

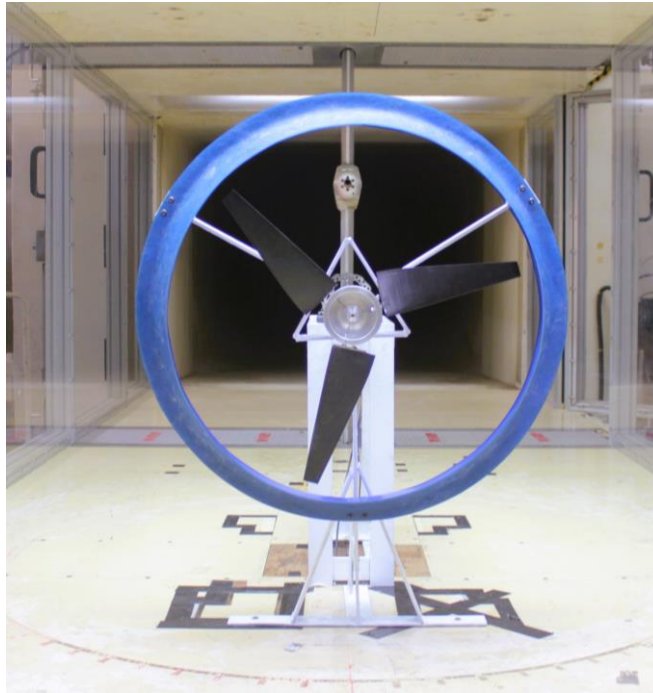


**Fig. 3. The 3-blade DAWT model inside the wind tunnel testing section.**

### **Blockage correction**

The blockage ratio of the 3-blade DAWT is 6.4%. Maskell correction was used for the diffuser shroud because it is suitable for configuration like a flat plate, Eq. (1) [35]. Because the rotor blade blockage is modest; only 1.4%, Pope and Harper's general formula is proper for the turbine blade correction [36], Eq. (2).

**(a) Maskell's correction:**

$$U = U\sqrt{1/(1 - mB_R)} \quad (1)$$

**(b) Pope & Harper Correction:**

$$U = U(1 + \epsilon_t) \quad (2)$$

where  $\epsilon_t = \frac{1}{4} B_R$ , and

$B_R$  (Blockage Ratio) = Model Projected Area/Wind tunnel Area

and  $m =$  Semi-empirical term=3.15.

### **5. Results and Discussion**

The performance of the 3-blade DAWT is shown in Fig. 4; the power coefficient curve is plotted using both CFD and wind tunnel. The wind tunnel results are presented after applying the blockage correction to the inlet speed. Both wind tunnel and CFD results match each other close to the design point of the DAWT. The maximum power coefficient of the 3-blade DAWT is 0.599.

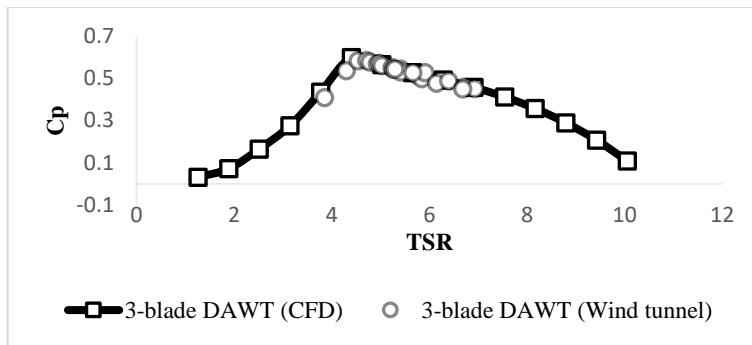


**Fig. 4. Power coefficient vs. TSR curve of both the 3-blade DAWT using CFD and wind tunnel**

### 5.1. Performance of the 2-blade DAWT vs. 3-blade DAWT using CFD

Figure 5 shows the power coefficient curve of the 3-blade final DAWT and the 2-blade final DAWT. The following could be seen:

- At high RPM (TSR), the 2-blade has better performance. The 2-blade DAWT has a 22% higher power than the 3-blade DAWT at TSR 7.5.
- At low RPM (TSR), the 3-blade has better performance. The 3-blade DAWT has 55.5% higher power than the 2-blade DAWT at TSR 4.39.
- The maximum power coefficient of the final 3-blade DAWT is 0.599, and the maximum power coefficient of the final 2-blade DAWT is 0.506.

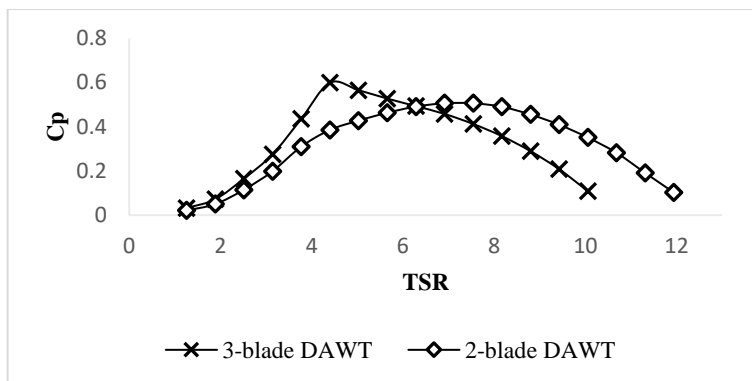


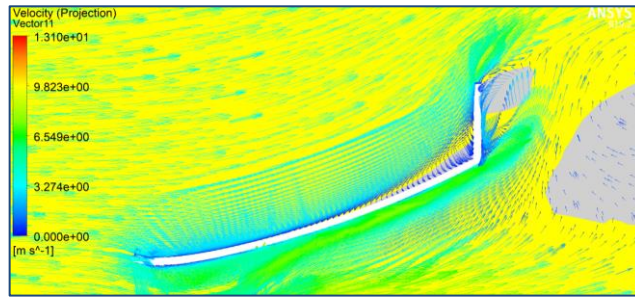
**Fig. 5. Cp vs. TSR curve of both the 3-blade and 2-blade using CFD.**

### 5.2. Insights of flow separation inside the diffuser

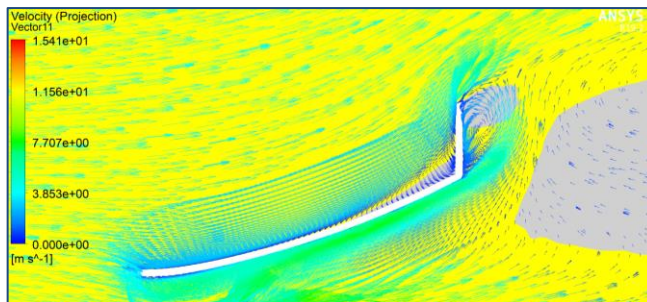
The flow behavior close to the diffuser wall can be explored by taking a cross-sectional plane across the DAWT. Figure 6 compares the flow structure inside the diffuser walls in the case of the 2-blade DAWT and 3-blade DAWT. The following point can be seen:

- The 3-blade DAWT at RPM 300 has the flow fully attached, then it separates at RPM 700 and then reattaches again at RPM 1100.

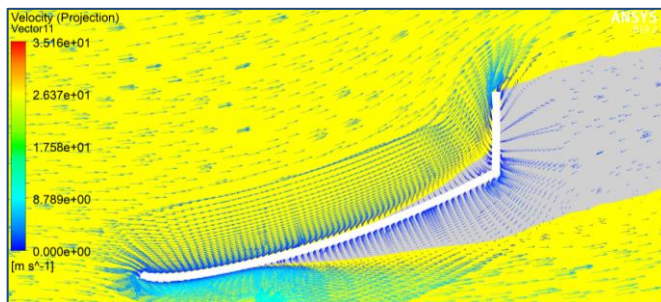
- The 2-blade DAWT at RPM 300 has the flow fully attached, then the flow separates at RPM 1100, and then reattaches partially at RPM 1700.



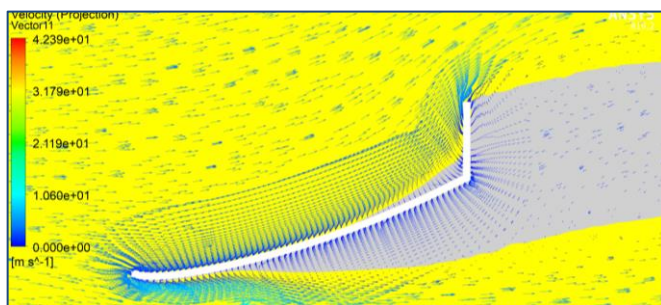
(a). RPM 300 (3-blade DAWT).



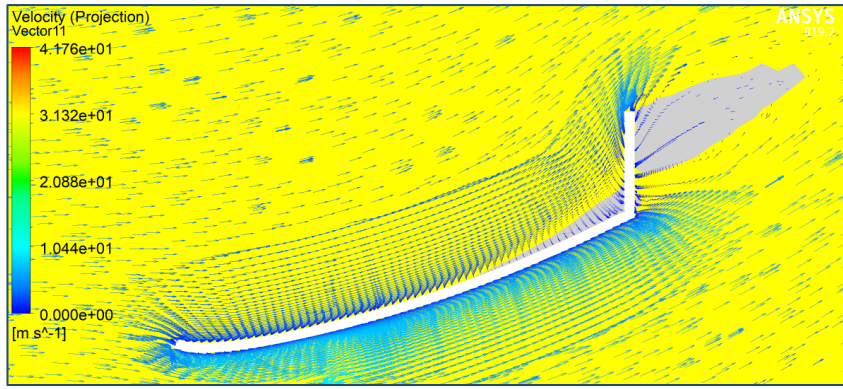
(b). RPM 300 (2-blade DAWT).



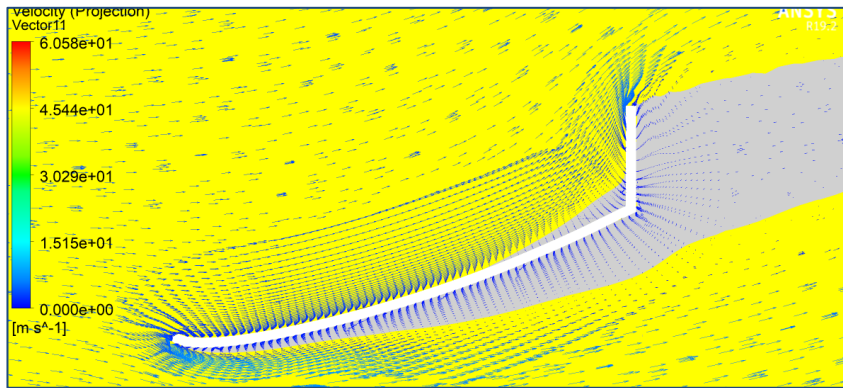
(c). RPM 700 (3-blade DAWT).



(d). RPM 1100 (2-blade DAWT).



(e). RPM 1100 (3-blade DAWT).



(f). RPM 1700 (2-blade DAWT).

**Fig. 6. Velocity vectors and flow separation (3-blade DAWT vs. 2-blade DAWT).**

The RPM of the rotor and the blade number influence the pattern of the separation, Fig. 6. Hence it is essential to calculate the rotor's velocity deficit across the rotor to understand the interaction between the rotors and the flow across the diffuser and how it influences the separation pattern. Table 4 shows the velocity deficit ratio across the rotor. The velocity deficit stands for the difference between the average velocity between the two planes shown in Fig. 7. The two planes are placed at 0.5D from the rotor's plane.

**Table 4. Percentage of velocity deficit between the inlet and outlet planes.**

RPM	3-blade DAWT			2-blade DAWT		
	300	700	1100	300	1100	1700
<b>Inlet plane</b>						
Average velocity (m/s)	4.75	4.652	4.5	4.817	4.7	4.785
<b>Outlet plane</b>						
Average velocity (m/s)	3.6	2.54	2.2	4.47	3.43	3.26
Velocity deficit (%)	24.2	45.4	51.1	7.2	27.0	31.9

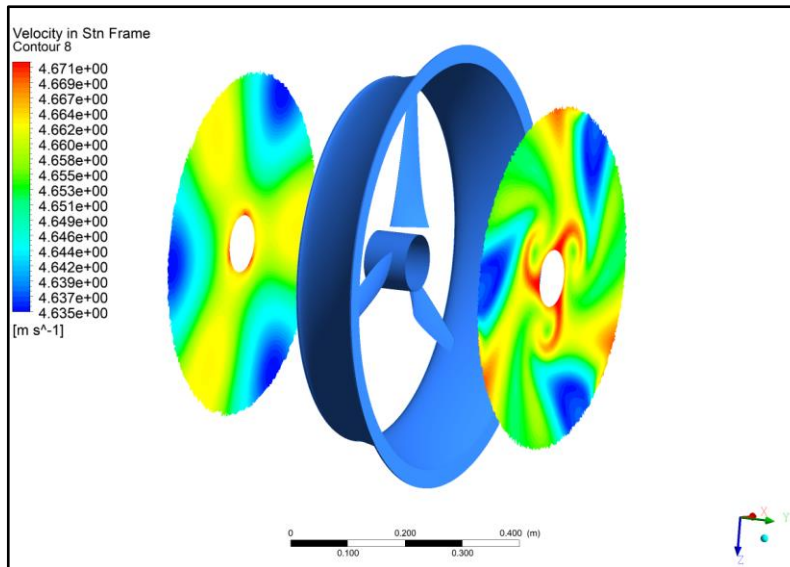


**Fig. 7. Velocity deficit between inlet and outlet planes.**

By looking at the pressure contours in Fig. 5 and the velocity deficit calculation, Table 4, the following can be seen in the case of the 3-blade DAWT:

- At RPM 300 (TSR 1.8): only small power is extracted, as previously illustrated in Fig. 5. The velocity deficit ratio is low (24% deficit), which means the wake's energy behind the rotor is still high and was used to energize the BL. Hence the BL is fully attached to the inner wall of the diffuser.
- At RPM 700 (TSR 4.39): The maximum output power is extracted at this operating point, as previously illustrated in Fig. 5. Low energy is left in the wakes behind the rotor (large velocity deficit ratio), which could not help the flow to attach to the walls.
- At RPM 1100: The torque extracted at this point approximates half the torque extracted at RPM 700. At the same time, the velocity deficit is slightly higher compared to the RPM 700 case. The small output torque and the large velocity deficit ratio mean that part of the energy is used to energize the BL to attach to the diffuser, as shown in Fig. 5.

By seeing the pressure contours in Fig. 6 and velocity deficit calculation as shown in Fig. 7, the following can be seen in the case of the 2-blade DAWT:

- At RPM 300, the velocity deficit ratio across the rotor is small, as shown in Table 4. Enough energy is left in the wake to energize the flow. Hence the flow is fully attached.
- At RPM 1100: the maximum torque is extracted at this point, leading to a large velocity deficit ratio, and hence the flow is separated.
- At RPM 1700: The extracted power is reduced compared to the power extracted at RPM 1100. Also, the velocity deficit ratio is smaller than at RPM 1100. The wake has more energy than the case at RPM 1100, making the flow start to reattach partially, as shown in Fig. 6.

### 5.3. Comparison of the flow structure of the 3-blade DAWT and 2-blade DAWT at RPM 1100

Comparison between the 2-blade DAWT and 3-blade DAWT cases at RPM 1100 because at this point, both cases have an approximate output power, as previously shown in Fig. 5. However, the flow behavior is different, as shown in Fig. 6.

The velocity deficit ratio of the 2-blade DAWT is small, but the flow still separates from the diffuser walls. Compared to the 3-blade DAWT, the flow is still attached at the same RPM. This observation shows that the number of blades is essential to energize the boundary layer at the diffuser walls.

Figure 8 depicts the velocity contours at the blade tips of the 3-blade DAWT and the 2-blade DAWT to further investigate the prior observation. At the blade tip, the average velocity is calculated. The tip of the 3-blade DAWT has more kinetic energy than the tip of the 2-blade. The 3-blade DAWT has an average velocity of 6.688 m/s, while the 2-blade DAWT has an average velocity of 5.015 m/s. It is concluded that adding more blade help add energy to the BL, which help attach to the diffuser's inner walls. This conclusion raises an extra point of interest, i.e., studying the flow behavior after adding an extra blade to the 3-blade DAWT. Section 5.5 shows if the 4-blade DAWT can help solve the separation problem.

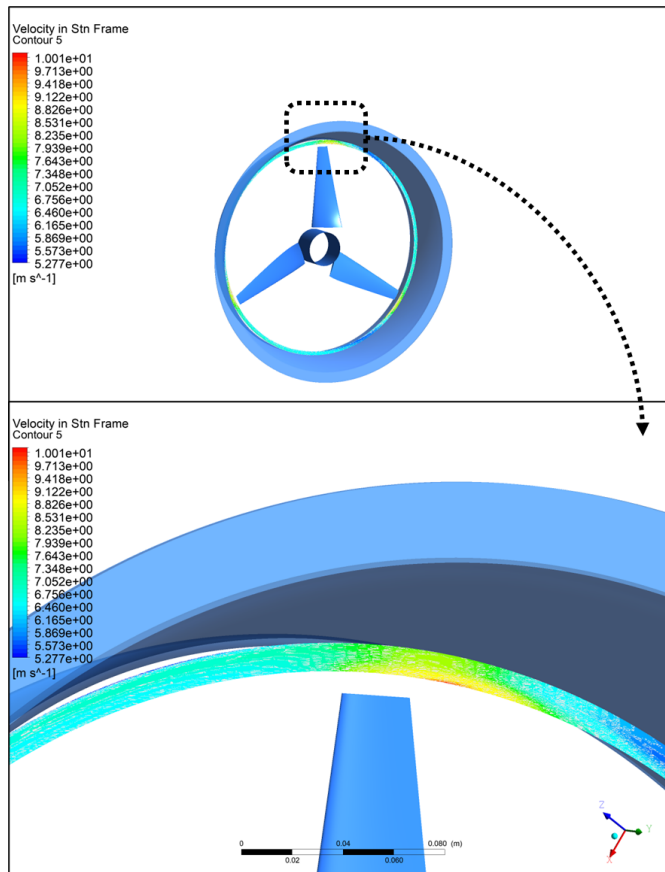


Fig. 8. Velocity contours at the blade tip.

### 5.4. Influence of the blade number on flow separation (using blade number as boundary layer controller)

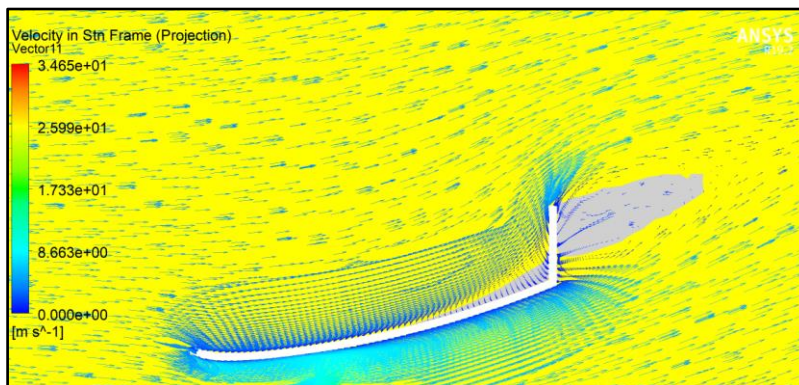
This section examines the possibility of using the blade’s number as a passive boundary layer controller. Figure 9 compares the flow structure of the 2-blade DAWT, the 3-blade DAWT, and the 4-blade DAWT at the RPM, which corresponds to the maximum power. The flow is vulnerable to separation at the maximum power, as mentioned in section 5.3. The opening angle is set at 10°, 15°, and 20°.

- At an opening angle of 10°: The 2-blade DAWT, the 3-blade DAWT, and the 4-blade DAWT have the flow fully attached to the inner surface of the diffuser.
- At an opening angle of 15°: The 2-blade DAWT has the flow fully separated, and the 3-blade DAWT has the flow partially separated. While the 4-blade DAWT still has the flow fully attached.
- At an opening angle of 20°: The 2-blade DAWT and 3-blade DAWT have the flow completely separated from the inner surface of the diffuser. The 4-blade DAWT still has the flow fully attached to the diffuser.
- The 4-blade DAWT has the flow fully attached in the three opening angles studied.

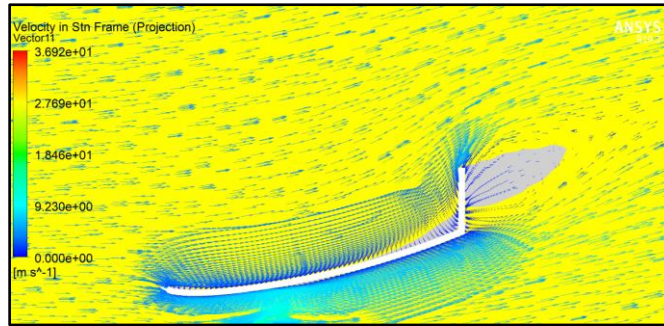
Table 5 shows that the 3-blade DAWT still has higher maximum output power than the 4-blade DAWT, with a small margin (less than 4%). However, the 4-blade DAWT has a better flow structure than the 3-blade because the boundary layer is permanently attached to the diffuser, which means that the 4-blade DAWT takes full advantage of the diffuser profile. It can be concluded in this section that increasing the number of blades can energize the inner flow and help it to attach to the inner surface of the diffuser. Hence the assumption that the rotor’s blade number and solidity can be used as a passive boundary layer controller is proved.

**Table 5. Maximum output power of the multi-blade final DAWT.**

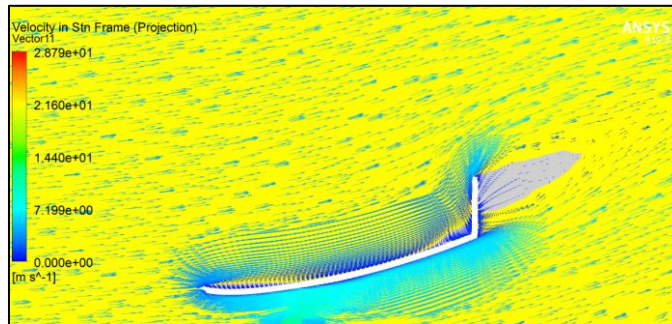
	10°	15°	20°
<b>2-blade</b>	11.56 W	10.96 W	10.37 W
<b>3-blade</b>	12.32 W	12.91 W	12.1 W
<b>4-blade</b>	11.06 W	11.89 W	12.41 W



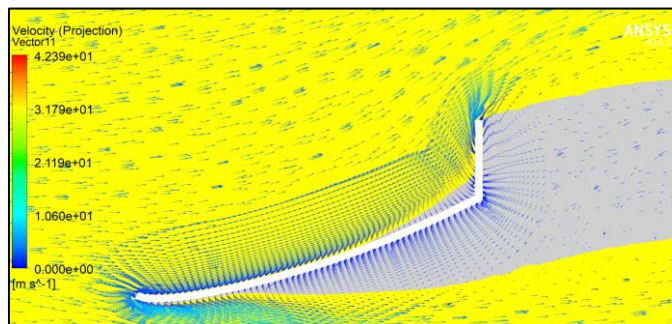
**(a). 10°/2-blade DAWT/RPM 1100.**



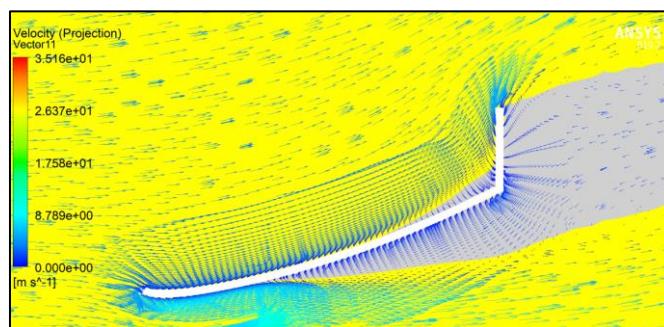
(b). 10°/3-blade DAWT/RPM 700.



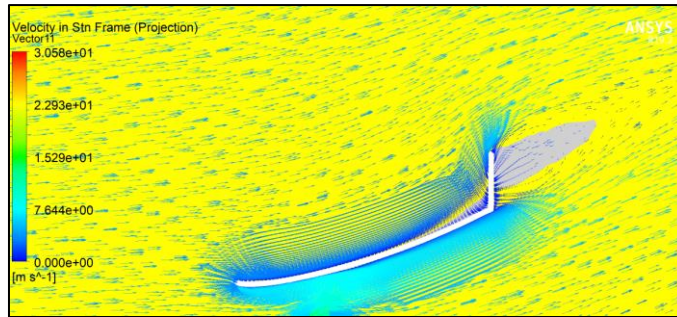
(c). 10°/4-blade DAWT/RPM 600.



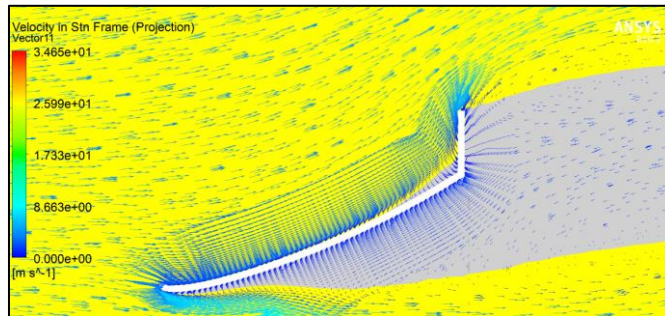
(d). 15°/2-blade DAWT/RPM 1100



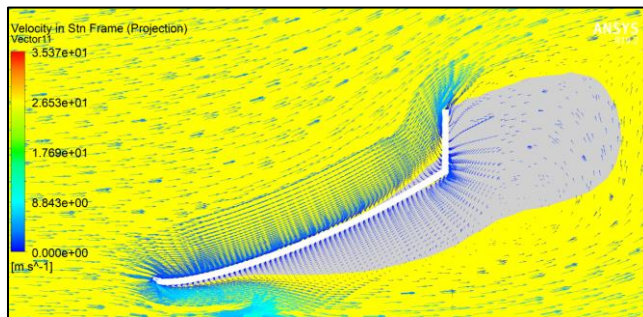
(e). 15°/3-blade DAWT/RPM 700.



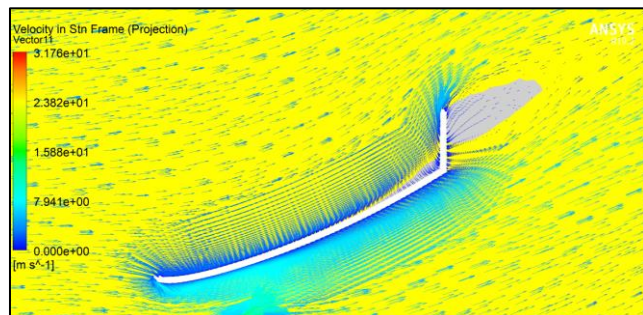
(f). 15°/4-blade DAWT/RPM600.



(g). 20°/2-blade DAWT/RPM 1100.



(h). 20°/3-blade DAWT/RPM 700.



(i). 20°/4-blade DAWT/RPM600

Fig. 9. Velocity vectors and flow separation.

## 6. Conclusions

In this research, it was found that increasing the number of the rotor blades of a DAWT increases the kinetic energy at the tip of the blades which energized the boundary layer inside the diffuser walls and consequently helps suppress the flow separation inside the inner wall of the DAWT. Velocity vectors from CFD results showed that the 4-blade DAWT has the flow fully attached to the diffuser at an opening angle of 20° compared to the 3-blade and 2-blade DAWT, which had the flow completely separated at the same opening angle. Hence it can be concluded that the number of blades can be used as a passive boundary layer control.

## 7. Future work

Findings of this research show that increasing the wake's energy at the rotor's tip can suppress the flow separation inside the inner walls of the DAWT, while findings from literature as discussed in section 2 shows that reducing the rotor's solidity can increase the augmentation ratio of the DAWT. The two mentioned goals cannot be achieved simultaneously using conventional blades. A possible way to achieve both benefits is to use truncated blades instead of conventional blades. The truncated rotors produced a jet-like flow in the wake with a high mean velocity at the tips [37]. Truncated rotors reduce solidity at the same time. Further investigation is required to find the influence of the trimmed blades on DAWT.

## Acknowledgments

The authors are grateful to Universiti Teknologi Malaysia (UTM) for providing valuable technical support to conduct this research project. The authors are also indebted to the UTM-Research University Grant, Tier 2 Vot Number Q.J130000.2651.16J33.

### Nomenclatures

$B_R$	Blockage Ratio
$C_p$	Power Coefficient
$m$	Semi-empirical term
$Y_{plus}$	Non-Dimensional distance

### Abbreviations

CFD	Computational Fluid Dynamics
DAWT	Diffuser Augmented Wind Turbine
RANS	Reynolds Average Navier Stokes
RPM	Revolutions Per Min
TSR	Tip Speed Ratio

## References

1. Aranake, A.C.; Lakshminarayan V.K.; and Duraisamy, K. (2014). Computational analysis of shrouded wind turbine configurations using a 3-dimensional RANS solver. *Renewable Energy*, 75, 818-832.

2. Ohya, Y.; Karasudani, T.; Nagai, T.; and Watanabe, K. (2017). Wind lens technology and its application to wind and water turbine and beyond. *Renewable Energy and Environmental Sustainability*, 2(2), 1-6.
3. Manwell, J.F.; McGowan, J.G.; and Rogers, A.L. (2009). *Wind energy explained: Theory, design and application*. (2<sup>nd</sup> ed.) Hoboken, New Jersey: Wiley.
4. Aranake, A.C.; Lakshminarayan, V.K.; and Duraisamy, K. (2013). Computational analysis of shrouded wind turbine configurations. *Proceedings of the 51st AIAA Aerospace Sciences Meeting including the New Horizons Forum and Aerospace Exposition*, Texas, USA, 1-17.
5. Toshimitsu, K.; Nishikawa, K.; Haruki, W.; Oono, S.; Takao, M.; and Ohya, Y. (2008). PIV measurements of flows around the wind turbines with a flanged-diffuser shroud. *Journal of Thermal Science*, 17(4), 375-380.
6. Ohya, Y. (2014). Bluff body flow and vortex - its application to wind turbines. *Fluid Dynamics Research*, 46(6), 61423- 61437.
7. Takeyeldein, M.M.; Lazim, T.M.; Ishak, I.S.; Nik Mohd, N.A.R.; and Ali, E.A. (2020). Wind lens performance investigation at low wind speed. *Evergreen*, 7(4), 481-488.
8. Takeyeldein, M.M.; Ishak, I.S.; and Lazim, T.M. (2022). Wind-lens turbine design for low wind speed. *Wind and Structures*, 35(3), 147-155.
9. Mühle, F.; Adaramola, M.S.; and Sretran, L. (2016). The effect of the number of blades on wind turbine wake - a comparison between 2-and 3-bladed rotors. *Journal of Physics: Conference Series*, 753, 032017-032027.
10. McLean, D. (2012). *Understanding aerodynamics: arguing from the real physics*. (1<sup>st</sup> ed). Wiley-Blackwell.
11. Ohya, Y.; Karasudani, T.; Sakurai, A.; and Inoue, M. (2006). Development of a high-performance wind turbine equipped with a brimmed diffuser shroud. *Transactions of the Japan Society for Aeronautical and Space Sciences*, 49(163), 18-24.
12. Watanabe, K.; and Ohya, Y. (2021). A simple theory and performance prediction for a shrouded wind turbine with a brimmed diffuser. *Energies*, 14(12), 3661.
13. Phillips, D.G.; Flay, R.G.J.; and Nash, T.A. (1998). Aerodynamic analysis and monitoring of the Vortec 7 diffuser-augmented wind turbine. *IPENZ Transactions*.Wellington, 26, 13-19.
14. Bontempo, R.; and Manna, M. (2014). Performance analysis of open and ducted wind turbines. *Applied Energy*, 136, 405-416.
15. Igra, O. (1976). Shrouds for aerogenerators. *AIAA Journal*, 14(10), 1481-1483.
16. Gilbert, B.L.; Oman, R.A.; and Foreman, K.M. (1978). Fluid dynamics of diffuser-augmented wind turbines. *Journal of Energy*, 2(6), 368-374.
17. Gaden, D.L.F.; and Bibeau, E.L. (2010). A numerical investigation into the effect of diffusers on the performance of hydro kinetic turbines using a validated momentum source turbine model. *Renewable Energy*, 35(6), 1152-1158.
18. Ohya, Y.; and Karasudani, T. (2010). A shrouded wind turbine generating high output power with wind-lens technology. *Energies*, 3(4), 634-649.

19. Anderson, J.D. (2021). *Modern compressible flow with historical perspective*. (4<sup>th</sup> ed). Boston: McGraw-Hill.
20. Bontempo, R.; and Manna, M. (2020). Diffuser augmented wind turbines: Review and assessment of theoretical models. *Applied Energy*, 280, 115867-115889.
21. Nunes, M.M.; Mendes, R.C.F.; Oliveira, T.F.; and Brasil Junior, A.C.P. (2020). Systematic review of diffuser-augmented horizontal-axis turbines. *Renewable and Sustainable Energy Reviews*, 133, 110075-110097.
22. Shonhiwa, C.; and Makaka, G. (2016). Concentrator augmented wind turbines: a review. *Renewable and Sustainable Energy Reviews*, 59, 1415-1418.
23. Jabbar Al-Quraishi, B.A.; Asmuin, N.Z.B.; Mohd, S.B.; Abd al-wahid, W.A.; Mohammed, A.N.; and Didane, D.H. (2019). Review on diffuser augmented wind turbine (DAWT). *International Journal of Integrated Engineering*, 11(1), 178-206.
24. Schubel, P.J.; and Crossley, R.J. (2012). Wind turbine blade design. *Energies*, 5(9), 3425-3449.
25. Wang, S.H.; and Chen, S.H. (2008). Blade number effect for a ducted wind turbine. *Journal of Mechanical Science and Technology*, 22(10), 1984-1992.
26. Chen, T.Y.; Liao, Y.T.; and Cheng, C.C. (2012). Development of small wind turbines for moving vehicles: Effects of flanged diffusers on rotor performance. *Experimental Thermal and Fluid Science*, 42, 136-142.
27. Abdelwaly, M.; El-Batsh, H.; and Hanna, M.B. (2019). Numerical study for the flow field and power augmentation in a horizontal axis wind turbine. *Sustainable Energy Technologies and Assessments*, 31, 245-253.
28. Asl, H.A.; Monfared, R.K.; and Rad, M. (2017). Experimental investigation of blade number and design effects for a ducted wind turbine. *Renewable Energy*, 105, 334-343.
29. Riyanto; Pambudi, N.A.; Febriyanto, R.; Wibowo, K.M.; Setyawan, N.D.; Wardani, N.S.; Saw, L.H.; and Rudiyanto, B. (2019). The performance of shrouded wind turbine at low wind speed condition. *Energy Procedia*, 158, 260-265.
30. Nunes, M.M.; Mendes, R.C.F.; Oliveira, T.F.; and Brasil Junior, A.C.P. (2019). An experimental study on the diffuser-enhanced propeller hydrokinetic turbines. *Renewable Energy*, 133, 840-848.
31. Agha, A., Chaudhry, H.N., and Wang, F. (2020). Determining the augmentation ratio and response behaviour of a Diffuser Augmented Wind Turbine (DAWT). *Sustainable Energy Technologies and Assessments*, 37, 100610-100630.
32. Ohya, Y.; Karasudani, T.; Sakurai, A.; Abe, K.; and Inoue, M. (2008). Development of a shrouded wind turbine with a flanged diffuser. *Journal of Wind Engineering and Industrial Aerodynamics*, 96(5), 524-539.
33. Toshimitsu, K.; Kikugawa, H.; Sato, K.; and Sato, T. (2012). Experimental investigation of performance of the wind turbine with the flanged-diffuser shroud in sinusoidally oscillating and fluctuating velocity flows. *Journal of the Japan Society of Mechanical Engineers*, 2(4), 215-221.

34. Agha, A.; Chaudhry, H.N.; and Wang, F. (2018). Diffuser augmented wind turbine (DAWT) technologies: a review. *International journal of Renewable Energy Research*, 8, 1369-1385.
35. Jeong, H.; Lee, S.; and Kwon, S.D. (2018). Blockage corrections for wind tunnel tests conducted on a Darrieus wind turbine. *Journal of Wind Engineering and Industrial Aerodynamics*, 179, 229-239.
36. Barlow, J.B.; Rae, W.H.; and Pope, A. (1999). *Low-speed wind tunnel testing*. (3<sup>rd</sup> ed). Wiley.
37. Cheng, S.; Jin, Y.; and Chamorro, L.P. (2020). Wind turbines with truncated blades may be a possibility for dense wind farms. *Energies*, 13(7),1810-1823.